

H-ARAIM Exclusion: Requirements and Performance

Yawei Zhai and Boris Pervan
Illinois Institute of Technology

Mathieu Joerger
The University of Arizona

BIOGRAPHY

Yawei Zhai obtained a Bachelor degree in Mechanical Engineering from Qingdao University of Science and Technology, China, in 2013. He is currently a PhD candidate and Research Assistant in Mechanical and Aerospace Engineering at Illinois Institute of Technology (IIT). His research focuses on ground and airborne monitors for advanced receiver autonomous integrity monitoring (ARAIM) using multi-constellation global navigation satellite systems.

Dr. Mathieu Joerger obtained a Diplôme d'Ingénieur in Mechatronics from the Ecole Nationale Supérieure des Arts et Industries de Strasbourg, France, in 2002, and a M.S. and a Ph.D. in Mechanical and Aerospace Engineering from the Illinois Institute of Technology (IIT), in 2002 and 2009 respectively. He is the 2009 recipient of the Institute of Navigation (ION) Parkinson award, and the 2014 recipient of the ION's Early Achievement Award. He is currently an assistant professor at The University of Arizona, working on multi-sensor integration, on sequential fault-detection for multi-constellation navigation systems, and on relative and differential receiver autonomous integrity monitoring (RAIM).

Dr. Boris Pervan is a Professor of Mechanical and Aerospace Engineering at IIT, where he conducts research on advanced navigation systems. Prior to joining the faculty at IIT, he was a spacecraft mission analyst at Hughes Aircraft Company (now Boeing) and a postdoctoral research associate at Stanford University. Prof. Pervan received his B.S. from the University of Notre Dame, M.S. from the California Institute of Technology, and Ph.D. from Stanford University. He is an Associate Fellow of the AIAA, a Fellow of the Institute of Navigation (ION), and Editor-in-Chief of the ION journal NAVIGATION. He was the recipient of the IIT Sigma Xi Excellence in University Research Award (2011, 2002), Ralph Barnett Mechanical and Aerospace Dept. Outstanding Teaching Award (2009, 2002),

Mechanical and Aerospace Dept. Excellence in Research Award (2007), University Excellence in Teaching Award (2005), IEEE Aerospace and Electronic Systems Society M. Barry Carlton Award (1999), RTCA William E. Jackson Award (1996), Guggenheim Fellowship (Caltech 1987), and Albert J. Zahm Prize in Aeronautics (Notre Dame 1986).

ABSTRACT

Future dual-frequency, multi-constellation advanced receiver autonomous integrity monitoring (ARAIM) is expected to bring significant navigation performance improvement to civil aviation. Horizontal ARAIM (H-ARAIM) is intended to serve one of the two operational scenarios that are currently being investigated in ARAIM. H-ARAIM aims at providing horizontal navigation for aircraft en-route, terminal, initial approach, non-precision approach (NPA) and departure operations. This paper discusses navigation requirements for those operations, describes a fault detection and exclusion (FDE) algorithm, and analyzes H-ARAIM availability performance. The paper is organized in three parts. In the first part, integrity and continuity requirements are described and interpreted for H-ARAIM operations. This paper shows that H-ARAIM exclusion is needed to achieve the required continuity. Accordingly, we derive a complete continuity risk equation which accounts for all sources of loss of continuity (LOC). The second part of the paper provides a step-by-step description of the FDE algorithm, establishes a predictive integrity risk bound, and quantifies the tightness of this bound. The core of this algorithm is exclusion function, which is designed to identify and remove the fault when detection occurs, thereby improving continuity. In the last part of the paper, H-ARAIM availability performance is analyzed using a baseline GPS/GALILEO constellation. The results indicate that implementing exclusion can significantly improve H-ARAIM continuity, and achieve high availability in the meanwhile. Moreover, a critical satellite analysis is carried out in this part to account for

the impact of unscheduled satellite outages (USO) on continuity. We point out that this impact is noticeable at some locations on earth and propose a method to resolve this issue.

INTRODUCTION

Global navigation satellite system (GNSS) measurements are vulnerable to faults including satellite and constellation failures, which can potentially lead to major integrity threats for users. To mitigate their impact, fault detection algorithms, such as receiver autonomous integrity monitoring (RAIM), can be implemented [1, 2]. The core principle of RAIM is to exploit redundant measurements to achieve self-contained fault detection at the user receiver [3].

With the modernization of GPS, the full deployment of GLONASS, and the emergence of Galileo and Beidou, a greatly increased number of redundant measurements becomes available, which has recently led to a renewed interest in RAIM. In particular, due to its potential to achieve worldwide coverage of guidance with a reduced investment in ground infrastructure, dual-frequency, multi-constellation advanced RAIM (ARAIM) has attracted considerable attention in the European Union and the United States [4, 5].

Currently, two versions of ARAIM corresponding to two operational scenarios are being investigated: horizontal ARAIM (H-ARAIM) aims at providing horizontal navigation integrity for aircraft en-route, terminal, initial approach, non-precision approach (NPA) and departure operations, and vertical ARAIM (V-ARAIM) is intended for aircraft approach [6]. ARAIM is scheduled to first provide horizontal service with improved availability performance as compared to existing RAIM [6]. Therefore, H-ARAIM is of primary interest and it is the focus of this paper.

RAIM became operational in the mid-90s as a backup navigation tool to support aircraft en-route flight using GPS only [7]. H-ARAIM may be considered an evolution of RAIM that takes advantage of GNSS modernization and of newly deployed GNSS. H-ARAIM also serves for operations with more stringent navigation requirements. For example, horizontal alert limit (HAL) as low as 0.1 nautical miles are considered for H-ARAIM NPA operations; in this case, when H-ARAIM is used as primary navigation tool, loss of continuity (LOC) becomes a more serious safety event. These differences in target level of safety must be accounted for in the design of H-ARAIM, and motivate the reassessment of fault detection and exclusion (FDE) method as compared to conventional RAIM.

While fault detection reduces integrity risk, fault exclusion can reduce continuity risk. The exclusion function is called once an alarm is triggered, and it autonomously identifies and removes the cause of the alarm, thereby preserving continuity of service. However, the gain in continuity comes at the cost of increased integrity risk [8, 9]. This is due to the fact that (a) excluding satellites may weaken the satellite geometry, and (b) the possibility of excluding the wrong satellite increases the integrity risk. Therefore, exclusion introduces a tradeoff between integrity and continuity. Whether the exclusion function is even needed or not depends on the operation. This is why this paper first discusses H-ARAIM navigation requirements.

This paper focuses on integrity and continuity requirements (other metrics are also specified in ARAIM [4, 6]). In particular, continuity is of primary concern in H-ARAIM. One reason for this is that when other, non-GNSS-based navigation tools (including visual beacons) are not available, LOC during H-ARAIM operations can lead the aircraft to be left without means of navigation. Given that the GPS constellation service provider (CSP) ensures a satellite fault rate lower than three per year [10], and assuming that other constellations perform similarly, this paper will show that detecting failures occurring at such a rate causes the continuity requirement to be exceeded. Therefore, exclusion is needed for H-ARAIM operations.

When exclusion is implemented, the following LOC sources are considered: not excluded false alarm (NEFA), not excluded fault detection (NEFD), unscheduled satellite outages (USO), radio frequency interference (RFI) and ionospheric scintillation (IOSC). To account for each individual contribution, the overall continuity risk budget is allocated to those five terms and each term is treated differently. The budget allocated to NEFA and NEFD respectively sets the detection and exclusion requirement. The probability of LOC due to USO can be quantified using a critical satellite analysis. In this paper, we assume that the impacts of RFI and IOSC on continuity are smaller than a predefined continuity risk allocation.

In the second part of this paper, a solution separation (SS) based FDE algorithm is designed and a practical implementation procedure is detailed. The exclusion function is performed in two steps. The first step determines the order of the exclusion candidates, based on the magnitudes of the SS detection test. In the second step, exclusion candidates are validated using a second layer detection, to confirm that the remaining measurements after exclusion are fault free. The test in this second step is carried out following the order defined in the first step. The first candidate that passes the validation test is the selected exclusion.

To evaluate the predictive integrity risk for the FDE algorithm, all causes for integrity threats are accounted for. The FDE integrity risk equation is derived as a weighted summation of all the exclusion options. However, a direct evaluation of the FDE integrity risk is challenging. In response, a conservative but computationally efficient upper bound is derived, based on the previous work in [9]. In this paper, we examine the tightness of the bound by comparing it to numerical values obtained using a Monte-Carlo (MC) simulation. Under circumstances detailed in the paper, substantial differences between the bound and the MC values are found, indicating the analytical bound can be loose. Also, a parity space representation is used to visualize what causes the bound to be overly-conservative.

The last part of the paper presents a performance analysis. Required navigation performance (RNP) 0.1 and RNP 0.3 are used as examples to show the achievable H-ARAIM performance (RNP 0.1 is the most stringent navigation requirement for H-ARAIM operations). Availability is evaluated using a baseline GPS/GALILEO combined constellation [6].

Two separate analyses are carried out: availability analysis and critical satellite analysis. By implementing the FDE algorithm described in the paper, the first analysis shows high availability performance can be achieved for both RNP 0.1 and 0.3. The second analysis indicates USO could have a significant impact on H-ARAIM continuity. In response, a potential approach to mitigate this issue is introduced in this paper.

NAVIGATION REQUIREMENTS

Among the metrics to measure navigation performance, this paper focuses on two most critical ones: integrity and continuity. The requirements for these two metrics are the same for H-ARAIM services, while RNP 0.1 and 0.3 correspond to two smallest HALs. Therefore, this work explores the H-ARAIM performance for RNP 0.1 and 0.3. In other words, if these two operations could be provided by H-ARAIM, the others can be achieved as well. Table 1 lists some key navigation parameters specified by international civil aviation organization (ICAO) [11], and each requirement is interpreted in details in this section.

Table 1. RNP 0.1 and 0.3 Navigation Requirements

	HAL	Integrity Risk I_{REQ}	Continuity Risk C_{REQ}
RNP 0.1	0.1nm (185m)	10^{-7} / hour	10^{-8} / hour to 10^{-4} / hour
RNP 0.3	0.3nm (556m)		

Integrity is a measure of trust that can be placed in the correctness of the information supplied by the total system [11]. Integrity risk is defined as the probability that an undetected navigation system error results in hazardous misleading information (HMI), which is the situation where the positioning error exceeds a predefined alert limit (AL). Since H-ARAIM only provides horizontal navigation service, only HAL needs to be considered.

HMI is considered as a *major* failure condition for H-ARAIM intended operations [12], and I_{REQ} is specified in a per hour basis. It is stated in [11] that H-ARAIM integrity risk requirement for a *single aircraft* is 10^{-5} / hour. Nevertheless, since GNSS based navigation could simultaneously serve a large number of aircraft over a large area, a system integrity failure could cause a much more serious consequence. To account for the impact of multiple aircraft, the value 10^{-7} / hour is used for H-ARAIM I_{REQ} .

In contrast with integrity, continuity is another crucial metric that measures the capability of the system to perform its function without unscheduled interruptions during the intended operation. Continuity risk, or probability of LOC, is the probability of a detected but unscheduled navigation function interruption after an operation has been initiated.

The occurrence of H-ARAIM LOC is also regarded as a *major* failure condition [12]. As shown in Table 1, continuity risk requirement is specified in a per hour basis in a range. This requirement is much more stringent in comparison with aircraft approach operations with vertical guidance, whose continuity risk requirements are normalized to a 15 second exposure time [13]. LOC during an approach leads the aircraft to abort the landing mission, go around, and try an approach again. But H-ARAIM missions cannot be easily aborted once started, because other navigation means must be found if LOC occurs during H-ARAIM operations. As a consequence, it increases the workload of the crews and brings stress to the air traffic controller (ATC). In particular, for the case when additional navigation methods are not available, H-ARAIM LOC could put the aircraft in a dangerous situation.

Similar to I_{REQ} , H-ARAIM C_{REQ} accounts for the impact on multiple aircraft. According to [11], the navigation system continuity requirement for a *single aircraft* is 10^{-4} / hour. But this requirement is flexible for satellite-based systems, depending on the traffic density and airspace complexity. For example, the most stringent requirement 10^{-8} / hour is suitable for the area where many aircraft use the same service and additional navigation tools are not available. The intermediate value 10^{-6} / hour could be used for the situations of high air traffic density and

airspace complexity, but the means to mitigate the LOC impact are present [11].

Unlike I_{REQ} , the specifications of C_{REQ} are slightly different over multiple aviation literatures. For example: [14] specifies C_{REQ} for en-route flight is 10^{-5} / hour and 10^{-6} / hour for lateral navigation only (LNAV) approach; [15] uses a different range of the continuity risk requirement from 10^{-7} / hour to 10^{-5} / hour. Therefore, the actual H-ARAIM C_{REQ} applied on the aircraft may be variable, and is highly dependent on the operation. For simulation purposes in this paper, the continuity requirement needs to be set in general, and consistent with most specifications. We use the following C_{REQ} value for H-ARAIM:

$$C_{REQ} = 10^{-6} / \text{hour} \quad (1)$$

Since C_{REQ} for a single aircraft is 10^{-4} / hour, equation (1) corresponds to the situation where 100 aircraft are simultaneously using the same GNSS navigation service, and possible mitigation means are available if a LOC occurs.

NEED OF H-ARAIM EXCLUSION

The need of exclusion can be assessed by examining the overall failure rate, and then comparing with the predefined continuity requirement [13]. Exclusion is required if the fault occurrence rate exceeds C_{REQ} . The GPS constellation is committed to having fewer than 3 faults per year, which corresponds to a fault rate of 10^{-5} / hour / satellite [10]. For the other constellations, we assume they can achieve the same satellite fault rate as GPS. As for the constellation failure rate, 0 can be used for GPS, but not for other constellations [16].

A typical example case for H-ARAIM is employed to analyze the impact of fault detection (FD) on LOC. The following assumptions are made in this analysis:

- two constellations are providing H-ARAIM service;
- there are 8 satellites in view from each constellation;
- the constellation failure rate is 10^{-4} / hour for the non-GPS constellation;
- a fault occurrence will result in detection and LOC.

Without airborne exclusion, the probability of LOC due to H-ARAIM FD can be computed:

$$\begin{aligned} P_{FD} &\gg 10^{-5} / \text{hour} / \text{SV} \cdot 16\text{SVs} + 10^{-4} / \text{hour} \\ &= 2.6 \cdot 10^{-4} / \text{hour} \gg C_{REQ} \end{aligned} \quad (2)$$

As indicated from equation (2), H-ARAIM FD probability is much larger than C_{REQ} . Therefore, to fulfill navigation continuity, airborne exclusion is required for H-ARAIM.

OVERALL H-ARAIM LOC

With exclusion being implemented, five sources that cause H-ARAIM LOC are considered: NEFA, NEFD, USO, RFI and IOSC. It is assumed that each source could impact all aircraft in the area, which is different from the assumption made for false alarm in [17]. This is because H-ARAIM assumes ephemeris and clock errors are dominating error sources, and their anomalies could cause false alarm simultaneously for all aircraft. Therefore, the H-ARAIM LOC equation for a single aircraft is:

$$P_{LOC} = P_{NEFA} + P_{NEFD} + P_{USO} + P_{RFI} + P_{IOSC} \quad (3)$$

Figure 1 provides a H-ARAIM continuity tree that expresses equation (3). The total continuity risk is specified in a per hour per aircraft basis. To meet the continuity requirement, a direct comparison between equation (3) and (1) must be established to confirm $P_{LOC} \leq C_{REQ}$.

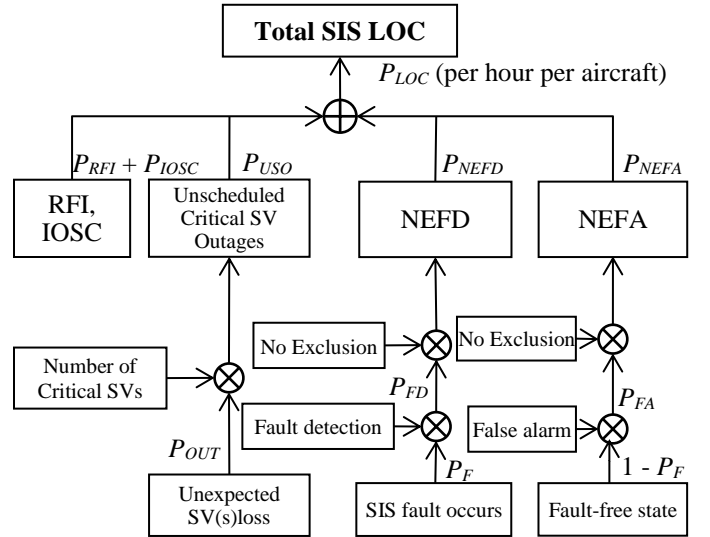


Fig. 1 H-ARAIM LOC Tree

In this work, an allocation of the total continuity requirement is made to account for these sources respectively. Thus, the H-ARAIM continuity requirement can be fulfilled as long as the probability of each event occurring is limited to be smaller than their allocated budget. Table 2 shows an example allocation of C_{REQ} , where the right column is the allocated budget for the corresponding event. This allocation is used in the H-ARAIM analysis in the remainder of this paper.

Table 2. Continuity Budget Allocation

$P_{NEFA,REQ}$	$4 \times 10^{-7} / \text{hour}$
$P_{NEFD,REQ}$	$4 \times 10^{-7} / \text{hour}$
$P_{USO,REQ}$	$10^{-7} / \text{hour}$
$P_{RFL,REQ} + P_{IOSC,REQ}$	$10^{-7} / \text{hour}$

P_{NEFA} is the probability of the occurrence of NEFA. Since H-ARAIM exclusion is implemented, the occurrence of a false alarm will trigger the exclusion function. Afterwards, only the alarms that cannot be excluded will result in LOC. This event could be quantified by equation (4) and bounded by equation (5):

$$P_{NEFA} = P(D_0, \bar{E} | H_0) P_{H_0} \quad (4)$$

$$< P(D_0 | H_0) P_{H_0} \quad (5)$$

where

D_0 : detection occurs using all-in-view satellites.

\bar{E} : no exclusion can be made.

H_0 : fault-free hypothesis, no fault existing.

P_{H_0} : prior probability of fault free case.

Equation (5) is the false alarm rate that can be used to set the detection threshold. Therefore, this event is controllable by the choice of detection threshold, and we can always guarantee $P_{NEFA} < P_{NEFA,REQ}$.

P_{NEFD} accounts for the LOC following an actual fault occurrence. Due to the exclusion function, FD would lead to continuity loss only if the fault cannot be excluded. Accordingly, limiting P_{NEFD} provides the requirement for the exclusion function.

$$P_{NEFD} = \sum_{i=1}^h P(D_0, \bar{E} | H_i) P_{H_i} \quad (6)$$

$$< \sum_{i=1}^h P(\bar{E} | H_i) P_{H_i} \quad (7)$$

where

H_i : multiple fault hypothesis, corresponds to fault mode from $i = 1 \dots h$, accounting for all faulty space vehicle (SV) combinations.

P_{H_i} : prior probability of the fault hypothesis.

Equation (7) is controllable by the choice of exclusion threshold so that the requirement for this event can be met, i.e., $P_{NEFD} < P_{NEFD,REQ}$.

P_{USO} accounts for the impact of unscheduled satellite outages on H-ARAIM continuity. A similar approach as used in the ground based augmentation system (GBAS) is employed here to quantify this impact [18]:

$$P_{USO} = n_c \cdot P_{out} \quad (8)$$

where

n_c : number of critical satellites, whose loss will result in LOC during an operation

P_{out} : probability of unscheduled satellite outages occurring, $P_{out} = 2 \times 10^{-4} / \text{hour} / \text{SV}$ [10].

The requirement of $P_{USO} \leq P_{USO,REQ}$ can be expressed in terms of n_c , i.e.:

$$n_c \leq \frac{10^{-7} / \text{hour}}{2 \times 10^{-4} / \text{hour} / \text{SV}} = 5 \times 10^{-4} \text{SVs} \quad (9)$$

Since the number of critical satellites must be an integer, equation (9) indicates that the number of critical satellite must be 0. In other words, the H-ARAIM continuity requirement is so stringent that it can only be met when there are no critical satellites. Therefore, a critical satellite analysis must be carried out for H-ARAIM.

At a specific location and time epoch, the following steps are employed to determine the number of critical satellites:

Step 1: Evaluate the integrity risk using all-in-view satellites. If the integrity risk is smaller than the requirement, then go to next step, otherwise, set $n_c = 0$.

Step 2: Remove one satellite and reevaluate the integrity risk. If the reevaluated integrity risk exceeds requirement, then the removed satellite is regarded as a critical satellite. Otherwise, it is not a critical satellite.

Step 3: Repeat step 2 for all the satellites. Record all the critical satellites.

Step 4: The number of critical satellites n_c is the summation of the critical satellites from step 3.

Determining n_c requires evaluation of integrity risk, so the H-ARAIM FDE algorithm and the method of quantifying its corresponding integrity risk are described in the next sections.

In this work, a continuity margin is left to account for the impact of RFI and IOSC. Because these two events are not quantified, we assume their contributions are always below the requirements.

FDE ALGORITHM DESCRIPTION

In this section, we provide a detailed, step-by-step description of a SS based FDE algorithm, with focus on the design of the exclusion function. Even though the motivation for developing this algorithm is to improve H-ARAIM continuity, the method could be extended into other applications.

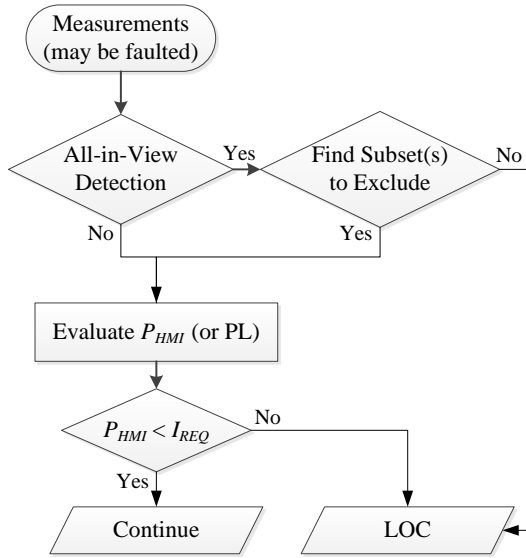


Fig. 2 FDE Algorithm Flow Diagram

Figure 2 is the flow diagram describing the FDE procedure in real time. This method originates from the SS ARAIM detection algorithm, which has been well defined and clarified [3, 5]. The additional exclusion steps are designed to identify the faulted satellite(s) to improve continuity when the measurements are faulted. For H-ARAIM applications, we assume that there are always enough measurement redundancies to exclude satellite fault. Also, since GPS constellation fault is 0, it could be used to exclude constellation fault even using dual-constellation H-ARAIM.

This algorithm can be summarized into 4 main steps:

- Step 1: Apply fault detection using all-in-view satellites. If there is no detection, go to step 4; if detection occurs, go to step 2.
- Step 2: Array the normalized detection statistics in a magnitude descending order. This order is called “exclusion option order”.

Step 3: Follow the order made in step 2, employ a *second layer detection test* for each option. The first option that passes this test is the final excluded one.

Step 4: Evaluate the real time integrity risk, or protection level (PL) using the present satellites. Then compare with the requirement to determine whether continue using GNSS.

At step 1, there are multiple test statistics associated with fault hypotheses. Using similar notations as our previous work [3, 9], the detection test statistic is defined as:

$$\Delta_d = \hat{x}_0 - \hat{x}_d = \varepsilon_0 - \varepsilon_d, \text{ for } d = 1 \dots h. \quad (10)$$

where

d : subscript of the number of detection test statistics, from 1... h ; the total number equals to the number of fault modes.

\hat{x}_0 : least squares position estimation using all-in-view satellites.

\hat{x}_d : least squares position estimate using satellites without the one(s) corresponding to fault mode d .

ε_0 : estimation error using all-in-view satellites, i.e., the difference between the estimated position and true position.

ε_d : estimation error using the satellite subset without the one(s) included in fault mode d .

To facilitate the exclusion procedure, all the detection statistics are normalized:

$$q_d = \frac{\Delta_d}{\sigma_{\Delta_d}} \text{ for } d = 1 \dots h. \quad (11)$$

where

σ_{Δ_d} : standard deviation of the solution separation test statistics Δ_d .

In the detection step, all the statistics in equation (11) are evaluated and compared with their corresponding thresholds T_d , which are predefined based on the navigation requirement. If *any* of the statistics exceed the threshold, an alarm is sent, indicating fault exists in the system. Otherwise, if *all* the statistics are smaller than the thresholds, the algorithm will go to the integrity risk evaluation step (the 4th step).

The second step is the start of the exclusion algorithm. When an alarm is sent, the normalized detection test statistics are arrayed in an order of descending magnitude, and the exclusion option order is determined based on that.

As a result, the first exclusion option corresponds to the fault hypothesis that results in the maximum statistic. This order will be followed when making exclusion attempts. The principle of choosing this order is due to the distributions of test statistics under a faulted condition. If an aircraft has encountered an actual fault, it is most likely that statistic corresponding to that fault mode is much larger than the others. A parity space representation is provided in next section to visualize this basis.

In the third step, the final exclusion option is made. It employs a second layer detection test to confirm there is no alarm in the satellite subset. The normalized second layer detection statistics are defined as:

$$q_{e,l} = \frac{\hat{x}_e - \hat{x}_{e,l}}{\sigma_{\Delta_{e,l}}} = \frac{\mathcal{E}_e - \mathcal{E}_{e,l}}{\sigma_{\Delta_{e,l}}}, \text{ for } l = 1 \dots h_e. \quad (12)$$

where

- e : subscript of the fault mode being excluded, $e = 1 \dots h$ for H-ARAIM.
- l : subscript of the number of the second layer detection test statistics, from $1 \dots h_e$; the total number is equal to the number of overall fault mode in the new satellite subset excluding e .
- \hat{x}_e : least squares position estimate using satellite subset excluding e .
- $\hat{x}_{e,l}$: least squares position estimate using new satellite subset after exclusion, except the one(s) in the second layer fault mode l .
- \mathcal{E}_e : estimation error using the satellite subset excluding e .
- $\mathcal{E}_{e,l}$: estimation error using the new satellite subset after exclusion, except the one(s) in the second layer fault mode l .
- $\sigma_{\Delta_{e,l}}$: standard deviation of the second layer detection test statistic $\Delta_{e,l}$.

This step goes through the exclusion options following the order determined in step 2. For each exclusion option, the second layer detection test is achieved by comparing each statistic in equation (12) with the corresponding threshold $T_{e,l}$ predefined by the navigation requirement.

If all the second layer statistics are within the thresholds, then the associated satellite(s) in the candidate fault mode is/are chosen to be excluded. However, it is possible that no exclusion can be made even after testing all the options. This case will result in LOC and it is accounted for in equation (6).

The fourth step evaluates the integrity risk (or PL) using the remaining satellites. The satellites being used in this step could be all-in-view satellites or satellite subsets after

exclusion steps. In real time, if the integrity risk (or PL) is below the requirement for the intended flight, then the GNSS position can be trusted. Otherwise, the aircraft has to stop using GNSS and switch to other navigation tools.

For this algorithm, steps 2 and 3 provide the mechanism of determining which satellite(s) to exclude. According to the design, two properties will result in a satellite subset to be excluded: there is no second layer detection after excluding this subset; this subset corresponds to the maximum detection statistic among the subsets that pass the second layer detection test. The remaining part of this section employs an illustrative example to help clarify this proposed algorithm.

Illustrative Example of FDE Algorithm

Assuming the following situation occurs in step 1 during an operation:

$$|q_1| \leq T_1, |q_2| \leq T_2, |q_3| > T_3, \dots |q_h| \leq T_h \quad (13)$$

Since an alarm is triggered, the exclusion function is called to remove this alarm. In the second step, all the detection statistics are arrayed in descending order. Assuming the following order is the result from step 2:

$$\text{descending magnitudes: } |q_3|, |q_7|, |q_1|, \dots |q_2| \quad (14)$$

$$\text{exclusion option order: } 1^{st}, 2^{nd}, 3^{rd}, \dots h^{th} \quad (15)$$

In the third step, the second layer detection test is made following the order of equation (15). The first exclusion option is excluding satellite(s) within fault mode 3. Assuming the second layer detection test for 3 is:

$$\text{first option: } |q|_{3,1} \leq T_{3,1}, |q|_{3,2} \leq T_{3,2}, \dots |q|_{3,h_e} \leq T_{3,h_e} \quad (16)$$

Since the first option passes the second layer detection test, then the final option is made by excluding satellites associated with fault mode 3. In this case, 3 corresponds to the maximum statistic in equation (14). Otherwise, if 3 does not pass the second layer test, this algorithm will attempt excluding satellites within fault mode 7.

SETTING FDE THRESHOLDS

With the FDE algorithm being available, the events of LOC described in the first part can be expressed using the test statistics and their thresholds. According to the allocated continuity budget, we are able to set the thresholds.

As described in the last section, detection occurs (D_0) when any of the first layer detection statistics exceeds the

thresholds, i.e.: $\bigcup_{d=1}^h |q_d| > T_d$. Also, an alarm cannot be excluded (\bar{E}) when no exclusion option can be made. In other words, the second layer detection occurs for all exclusion options: $\bigcap_{e=1}^h \left(\bigcup_{l=1}^{h_e} |q_{e,l}| > T_{e,l} \right)$.

Therefore, equation (5) can be written as:

$$P_{NEFA} < P \left(\bigcup_{d=1}^h |q_d| > T_d \mid H_0 \right) P_{H_0} \quad (17)$$

$$< \sum_{d=1}^h P \left(|q_d| > T_d \mid H_0 \right) P_{H_0} \leq P_{NEFA,REQ} \quad (18)$$

Based on the allocated $P_{NEFA,REQ}$, the first layer detection thresholds T_d for H-ARAIM can be computed:

$$T_d = Q^{-1} \left\{ \frac{P_{FA,NE,REQ}}{2P_{H_0} \cdot h} \right\} \quad (19)$$

where Q^{-1} is the inverse tail probability function.

Similarly, the thresholds of the second layer detection statistics are set based on $P_{NEFD,REQ}$. Equation (7) becomes:

$$P_{NEFD} < \sum_{i=1}^h P \left(\bigcap_{e=1}^h \left(\bigcup_{l=1}^{h_e} |q_{e,l}| > T_{e,l} \right) \mid H_i \right) P_{H_i} \quad (20)$$

$$< \sum_{i=1}^h P \left(\bigcup_{l=1}^{h_e} |q_{i,l}| > T_{i,l} \mid H_0 \right) P_{H_i} \quad (21)$$

$$< \sum_{i=1}^h \sum_{l=1}^{h_e} P \left(|q_{i,l}| > T_{i,l} \mid H_0 \right) P_{H_i} \leq P_{NEFD,REQ} \quad (22)$$

The bound from equation (20) to (21) is worth mentioning, where only one exclusion option associated with the fault hypothesis is considered, i.e., $e = i$. Since the fault is excluded, the second layer detection statistics in equation (21) are fault free (H_0). And then, equation (22) can be used to set the second layer detection thresholds over all the fault hypotheses. In this work, we use an even allocation of $P_{NEFD,REQ}$ into those hypotheses. Thus,

$$T_{i,l} = Q^{-1} \left\{ \frac{P_{NEFD,REQ,H_i}}{2 \cdot h_e} \right\}, \text{ where } P_{NEFD,REQ,H_i} = \frac{P_{NEFD,REQ}}{h \cdot P_{H_i}} \quad (23)$$

QUANTIFY PREDICTIVE FDE INTEGRITY RISK

In real time operation, the evaluation of integrity risk (or PL) in step 4 takes the knowledge of measurements. The receiver knows whether the exclusion step has been made or not, and which satellite subset is excluded. However, to predict H-ARAIM FDE availability, all the possible situations that the aircraft may encounter need to be characterized. This is why we account for all the exclusion options in the predictive integrity risk equation in our previous work [8, 9].

Corresponding to this ARAIM FDE algorithm, the predictive integrity risk equation should include all the possibilities that cause integrity threats:

$$P_{HMI} = P(HI_0, \bar{D}_0) + \sum_{j=1}^h P(HI_j, E_j, D_0) \quad (24)$$

where

HI_0 : hazardous misleading information using all-in-view satellites positioning: $|\mathcal{E}_0| > \ell$, where ℓ is the alert limit for the intended operation.

\bar{D}_0 : no fault detection using all-in-view satellites:

$$\bigcap_{d=1}^h |q_d| \leq T_d.$$

HI_j : hazardous misleading information in positioning using satellites except the one(s) being excluded: $|\mathcal{E}_j| > \ell$.

E_j : satellite(s) within fault mode j is chosen to be excluded. Two properties: no second layer

detection after excluding j (\bar{D}_j): $\bigcap_{l=1}^{h_e} |q_{j,l}| \leq T_{j,l}$; j

corresponds to the maximum detection statistic among the subsets that pass the second layer detection test (MAX_j): $\bigcap_{S_p \subset S_{pass}} |q_j| > |q_p|$, where

S_{pass} is the group composed of the exclusion options passing the second layer detection test, both j and p are within S_{pass} .

Employing the multiple fault hypothesis approach, equation (24) becomes:

$$P_{HMI} - P_{NM} < \sum_{i=0}^h \max_{f_i} \left(P(HI_0, \bar{D}_0 \mid H_i, f_i) + \sum_{j=1}^h P(HI_j, \bar{D}_j, MAX_j, D_0 \mid H_i, f_i) \right) P_{H_i} \quad (25)$$

In equation (25), P_{NM} accounts for the not monitored fault hypotheses whose prior probabilities are so small that there is no need to evaluate their corresponding

conditional integrity risk. Under a hypothesis H_i , f_i is the associated fault which can be fully described by the direction and magnitude [3]. The worst case fault \bar{f}_i is obtained when the conditional FDE integrity risk for H_i reaches maximum.

In the big bracket of equation (25), the causes of integrity threats for one hypothesis can be classified into three categories: no detection (ND), correct exclusion (CE) and wrong exclusion (WE). To clarify those categories, we introduce an example in this section which can be easily visualized in parity space.

Canonical Example

This example called ‘canonical example’ has been introduced in our previous work [3, 8, 9]. It has a simple measurement model:

$$\mathbf{z} = \mathbf{H}\mathbf{x} + \mathbf{v} + \mathbf{f} \quad (26)$$

where,

$$\mathbf{H} = [1 \ 1 \ 1]^T \text{ and } \mathbf{v} \sim N(\mathbf{0}_{3 \times 1}, \mathbf{I}_3) \quad (27)$$

Three fault hypothesis are considered for this model, corresponding to each measurement. Consider the hypothesis of H_1 , then the conditional FDE integrity risk is:

$$P_{HMI, H_1} = \max_{f_1} \left(\begin{array}{l} P(HI_0, \bar{D}_0 | H_1, f_1) \\ + P(HI_1, \bar{D}_1, MAX_1, D_1 | H_1, f_1) \\ + \sum_{j=2}^3 P(HI_j, \bar{D}_j, MAX_j, D_0 | H_1, f_1) \end{array} \right) P_{H_1} \quad (28)$$

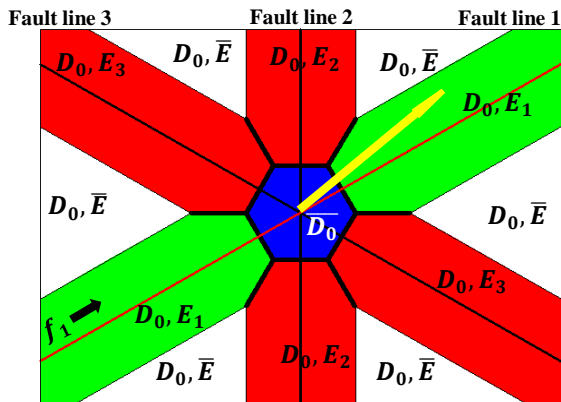


Fig. 3 Parity Space Representation of FDE Regions

In equation (28), three terms of the conditional integrity risk correspond to the three categories. And Figure 3 shows an associated 2-D parity space representation. This

space can be divided into four regions by the FDE algorithm and are demonstrated here using different colors. The yellow arrow is the parity vector in Figure 3, whose mean is along the fault line 1 in this case. The blue shaped hexagon is no detection region using SS approach. No alarm will trigger if the parity vector lies inside. The green region corresponds to correct exclusion. It covers the fault line that is the actual fault mode. The red areas represent wrong exclusion events, where the fault will be wrongly excluded if the parity vector lies in those regions. The white regions in Figure 3 correspond to no exclusion region: if the parity vector lies into the white area, the fault cannot be excluded and there will be a LOC event.

To evaluate the integrity risk of equation (28), the worst case fault \bar{f}_1 must be found. As shown in parity space, we need to vary the fault until the summed integrity risk from the three categories is maximized. However, this approach is cumbersome and very difficult to implement. In response, a practical approach was derived in our previous work [9], which provides an efficient way to bound the FDE integrity risk. The next sections clarify the bounding steps and investigate the tightness of the bound.

BOUND FDE INTEGRITY RISK

Two main conservative steps are used to bound equation (25) and steps are summarized using following equations:

$$\begin{aligned} P_{HMI} - P_{NM} &< \sum_{i=0}^h \max_{f_{i,0}} P(HI_0, \bar{D}_0 | H_i, f_{i,0}) P_{H_i} \\ &+ \sum_{i=0}^h \sum_{j=1}^h \max_{f_{i,j}} P(HI_j, \bar{D}_j, MAX_j, D_0 | H_i, f_{i,j}) P_{H_i} \\ &< \sum_{i=0}^h \max_{f_{i,0}} P(HI_0, \bar{D}_0 | H_i, f_{i,0}) P_{H_i} \\ &+ \sum_{i=0}^h \sum_{j=1}^h \max_{f_{i,j}} P(HI_j, \bar{D}_j | H_i, f_{i,j}) P_{H_i} \end{aligned} \quad (29)$$

Equation (29) provides a bound for equation (25), where the integrity risks for hypothesis H_i is maximized individually over each exclusion option. This approach treats the fault f_i differently whereas it is the same under one hypothesis. For example, $f_{i,0}$ corresponds to the fault of H_i for the case where no detection occurs. The integrity risk bound for this term can be obtained by varying $f_{i,0}$. Similarly, for the case where j is excluded, the integrity bound can be found by varying the fault $f_{i,j}$ for each term to maximize the conditional integrity risk.

Therefore, summing the maximized individual risks will always provide a bound than maximizing the summed risk.

In equation (30), two criteria in exclusion terms are eliminated: fault detection using all satellites D_0 and maximum detection test statistic MAX_j . This approach is adopted to simplify the computation load when evaluating the conditional integrity risk. There is a typical approach we use to bound equation (30) with SS method. Using the notations specified in previous sections, equation (30) can be written as:

$$P_{HMI} - P_{NM} < \sum_{i=0}^h \max_{f_{i,0}} P\left(|\varepsilon_0| > \ell, \bigcap_{d=1}^h |q_d| < T_d \mid H_i, f_{i,0}\right) P_{H_i} + \sum_{i=0}^h \sum_{j=1}^h \max_{f_{i,j}} P\left(|\varepsilon_j| > \ell, \bigcap_{l=1}^{h_l} |q_{j,l}| < T_{j,l} \mid H_i, f_{i,j}\right) P_{H_i} \quad (31)$$

The method of bounding equation (31) has been derived and fully described in [3, 9]. The final equation (32) distinguishes the FDE integrity risk from fault free state and faulted condition. All the variables in (32) have been defined and explained in this paper, and it can be used to bound the predictive H-ARAIM FDE integrity risk with a high computational efficiency.

$$P_{HMI} - P_{NM} < P\left(|\varepsilon_0| > \ell \mid H_0\right) P_{H_0} + \sum_{i=1}^h P\left(|\varepsilon_i| + \sigma_{\Delta_i} T_i > \ell \mid H_i\right) P_{H_i} + \sum_{j=1}^h P\left(|\varepsilon_j| > \ell \mid H_0\right) P_{H_0} + \sum_{i=1}^h \left(\sum_{\substack{j=1 \\ S_j=S_i}}^h P\left(|\varepsilon_j| > \ell \mid H_i\right) P_{H_i} + \sum_{\substack{j=1 \\ S_j=S_i}}^h P\left(|\varepsilon_{j,i}| + \sigma_{\Delta_{ji}} T_{j,i} > \ell \mid H_i\right) P_{H_i} \right) \quad (32)$$

However, due to the conservative steps, it is questionable whether the final equation provides a tight bound or not. In particular, unlike the typical SS approach from (31) to (32), the two steps in equation (29) and (30) are not investigated in previous work. In response, we express these two steps in parity space for the canonical example and perform an analysis on the tightness of the bound in this paper.

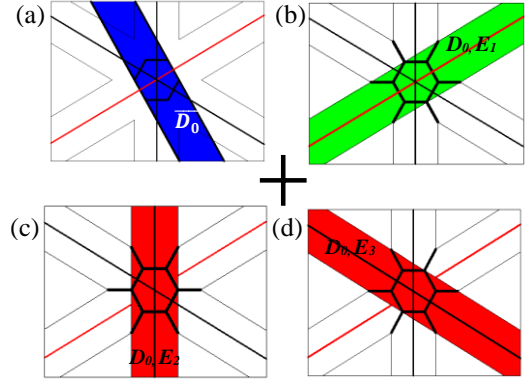


Fig. 4 Parity Space Representation of Bounding Regions for Each Term

Figure 4 demonstrates the bound of final equation (32) in parity space for the canonical example. In comparison with Figure (3), the integrity risks are maximized respectively for each term and summed up. This distinction is a reflection of the conservative step made in equation (29).

In figure 4, the subfigures (b), (c) and (d) correspond to the CE and WE events. Unlike Figure 3, those regions are overly bounded due to the elimination of the knowledge of MAX_j and D_0 in equation (30). As shown in (c) and (d), red regions pass through the fault line, whereas the actual wrong exclusion regions are away from the fault line in Figure 3. Since the mean of the parity vector is along the red lines as fault magnitude varies, the probability of it being in the red region at a hazardous state could dramatically increase. Therefore, equation (32) could be overly conservative for WE events.

TIGHTNESS OF THE FDE INTEGRITY RISK BOUND

This section aims at analyzing the tightness of the FDE integrity risk bound by comparing the results obtained using equation (32) and (25). Monte-Carlo (MC) simulation method is employed to numerically evaluate (25). The goal of this analysis is only to assess the tightness of the integrity bound, not to demonstrate H-ARAIM performance. Therefore, this analysis is only performed for the canonical example introduced in earlier sections.

In this analysis, the prior probability for each fault is assumed to be the same and the value is 10^{-3} . The false alarm requirement is set to be 10^{-6} . We run 10^7 trials and each trial follows the proposed FDE algorithm. In contrast, equation (32) is used to analytically compute the FDE integrity risk bound.

To investigate the sensitivity of the bound to navigation requirement, three levels of ALs: 3m, 4m and 5m are considered. For each level of AL, three cases corresponding to three exclusion requirements are explored:

$$P_{NEFD,REQ,H_i} = 10^{-1}, 10^{-3}, 10^{-5} \quad (33)$$

As a reminder, P_{NEFD,REQ,H_i} is the allocated exclusion requirement for each hypothesis shown in equation (23), and the exclusion thresholds can be set accordingly. Among the three cases, case 1 corresponds to $P_{NEFD,REQ,H_i} = 10^{-1}$, case 2 corresponds to 10^{-3} , and case 3 has the most stringent exclusion requirement, i.e., $P_{NEFD,REQ,H_i} = 10^{-5}$.

Table 3. P_{HMI} Results for Canonical Example

	AL = 3m		AL = 4m		AL = 5m	
	MC	Bound	MC	Bound	MC	Bound
Case 1	1.01×10^{-4}	1.3×10^{-3}	2.43×10^{-6}	7.37×10^{-5}	2.92×10^{-8}	1.91×10^{-6}
Case 2	1.03×10^{-4}	4.2×10^{-3}	4.03×10^{-6}	7.62×10^{-4}	7.45×10^{-7}	6.67×10^{-5}
Case 3	1.04×10^{-4}	7.3×10^{-3}	4.16×10^{-6}	2.7×10^{-3}	8.5×10^{-7}	4.6×10^{-4}

Table 3 shows the integrity risk results evaluated using MC simulation and the analytical bound, as a function of ALs and exclusion requirements. A big gap between these two results can be observed. Moreover, there is a big increase of the integrity risk evaluated by the analytical bound (values in blue boxes) as the exclusion requirement gets more stringent, whereas the numerical results only reflect a slightly increase.

To further demonstrate this difference, one specific case is used to investigate the contributions of integrity risk from the three categories: ND, CE and WE. The requirements $AL = 4$ and $P_{NEFD,REQ,H_i} = 10^{-3}$ are used for case.

Table 4. Integrity Risk of the Three Categories

	P(HI, \bar{D})		P(HI, CE, D)		P(HI, WE, D)	
	MC	Bound	MC	Bound	MC	Bound
H_0	0	4.3×10^{-12}	0	0	0	4.26×10^{-8}
H_1	7.27×10^{-4}	6.7×10^{-3}	0	1.54×10^{-8}	6.08×10^{-4}	0.12
H_2	7.23×10^{-4}	6.7×10^{-3}	0	1.54×10^{-8}	6.11×10^{-4}	0.12
H_3	7.32×10^{-4}	6.7×10^{-3}	0	1.54×10^{-8}	6.11×10^{-4}	0.12

In Table 4, the first column represents the multiple hypotheses from fault free to each single failure condition. The values in table 4 are the integrity risks of the corresponding hypothesis and category. Among the three categories, the most significant difference of the integrity risk is for the WE event. One explanation for this outcome is made in the last section, showing that the elimination of MAX_j and D_0 could potentially cause the bound of WE term to be loose. Our further work would investigate the possibility of tightening the predictive FDE integrity risk by taking use of the knowledge of MAX_j and D_0 . The integrity risk is expected to be reduced, even though the improvement may come with higher computational load.

Refining the FDE algorithm and tightening the integrity risk are beyond the scope of this paper, and we will use the analytical approach in this work to investigate the H-ARAIM performance. This is because the analytical approach of equation (32) is computationally efficient, and it always guarantees safety.

PERFORMANCE ANALYSIS OF H-ARAIM FDE

Having discussed the H-ARAIM navigation requirements and described the FDE algorithm, as well as the method to evaluate the predictive integrity risk, this part focuses on the H-ARAIM FDE performance analysis for two intended operations: RNP 0.1 and 0.3.

Two separate analyses are carried out in this work: availability analysis and critical satellite analysis. The same simulation conditions specified in [6] are used to achieve the analyses. Dual-frequency baseline GPS/GALILEO constellation with nominal parameters are used, with some key parameters listed in Table 5 below.

Table 5. Simulation Parameters for H-ARAIM Simulation

Integrity Req. I_{REQ}	10^{-7} /hour
Continuity Req. C_{REQ}	10^{-6} /hour
HAL	185m / 556m
P_{sat}	10^{-5}
P_{const}	GPS: 10^{-8} / GAL: 10^{-4}
σ_{URA}	2.5m
b_{nom}	0.75m
Mask Angle	5 degrees
Time Step	10 mins
Coverage Range	Worldwide

H-ARAIM FDE Predictive Availability Performance

Availability is defined as the fraction of time the navigation system is usable before the operation is initiated. This analysis shows the FDE availability performance of the predictive integrity. In other words, if the FDE integrity risk (or PL) is smaller than the requirement, the service is available.

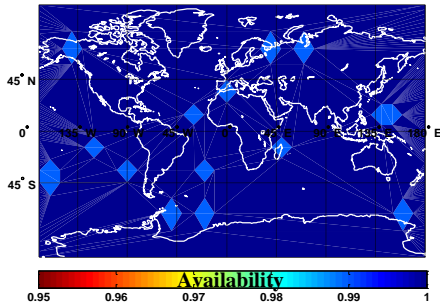


Fig. 5 H-ARAIM FDE Availability for RNP 0.1, Coverage (0.995 availability) = 97.53%

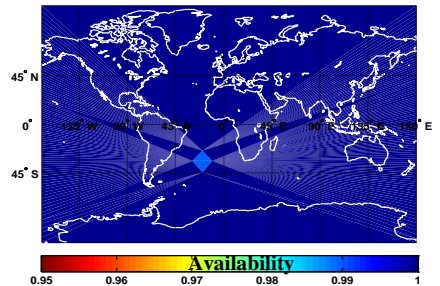


Fig. 6 H-ARAIM FDE Availability for RNP 0.3, Coverage (0.995 availability) = 99.98%

We can observe high coverage from both Figure 5 and 6, which corresponds to RNP 0.1 and 0.3 respectively. Therefore, by implementing the H-ARAIM FDE method provided in this paper, H-ARAIM continuity could be dramatically improved, along with achieving high availability performance.

H-ARAIM Critical Satellite Analysis

It has been shown in previous sections that H-ARAIM continuity requirement is so stringent that it does not allow for the existence of any critical satellites. This analysis assesses the number of critical satellites at all locations worldwide over a 1-day period. At one location, the number of critical satellite is averaged over time and then used to illustrate this impact worldwide.

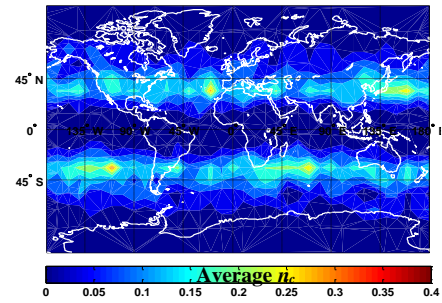


Fig. 7 Average n_c Map for RNP 0.1, Maximum number $n_{c,a,max} = 0.32$

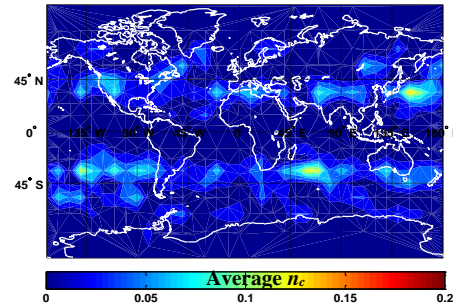


Fig. 8 Average n_c Map for RNP 0.3, Maximum number $n_{c,a,max} = 0.16$

Recall that the continuity requirement can be fulfilled only if $n_c = 0$. The results of Figure 7 and 8 show that the average critical satellite number is 0 at many locations, which indicates that the occurrence of USO would not lead to continuity loss. In contrast, there are also some locations where $n_c \neq 0$. So the occurrence of USO at those locations could have a noticeable impact on H-ARAIM continuity.

However, as discussed earlier, the critical satellite analysis results depend on the method of evaluating integrity. An upper bound that is used in this work could reduce the robustness to satellite geometry, and then declare a satellite to be ‘critical’ when it actually is not. Therefore, this impact may be mitigated by tightening the FDE integrity risk bound.

CONCLUSION

This paper explores the method of improving H-ARAIM continuity by implementing exclusion. There are three contributions of this work. First, we demonstrated the need of exclusion to meet H-ARAIM target navigation requirements, and we quantified H-ARAIM continuity. Second, we proposed an FDE algorithm, and evaluated the tightness of the corresponding analytically-derived predictive integrity risk bound. Third, the H-ARAIM availability performance was analyzed. Performance evaluations indicated that H-ARAIM continuity could be significantly improved using exclusion, while not

reducing availability substantially. Also, the impact of USO on H-ARAIM availability was quantified. In future work, we will investigate different approaches to tighten analytical integrity risk bounds for FDE algorithms, and we will apply these new approaches to analyze H-ARAIM availability performance.

ACKNOWLEDGEMENT

The authors would like to thank the Federal Aviation Administration for sponsoring this work. The views and opinions expressed in this paper are those of the authors and do not necessarily reflect those of any other organization or person.

REFERENCE

[1] Lee, Y. C., "Analysis of Range and Position Comparison Methods as a Means to Provide GPS Integrity in the User Receiver," *Proceedings of the 42nd Annual Meeting of The Institute of Navigation*, Seattle, WA, 1986, pp. 1-4.

[2] Parkinson, B. W., and Axelrad, P., "Autonomous GPS Integrity Monitoring Using the Pseudorange Residual," *NAVIGATION*, Washington, DC, Vol. 35, No. 2, 1988, pp. 225-274.

[3] M. Joerger, F.C. Chan, and B. Pervan, "Solution Separation Versus Residual-Based RAIM," *NAVIGATION*, Vol. 61, No. 4, Winter 2014, pp. 273-291.

[4] EU-U.S. Cooperation on Satellite Navigation, Working Group C, "ARAIM Technical Subgroup Interim Report, Issue 1.0," December 19, 2012. Available online at: http://ec.europa.eu/enterprise/newsroom/cf/getdocument.cfm?doc_id=7793

[5] J. Blanch, T. Walter, T. Lee, B. Pervan, M. Rippl, and A. Spletter, "Advanced RAIM User Algorithm Description: Integrity Support Message Processing, Fault Detection, Exclusion, and Protection Level Calculation," *Proc. of ION GNSS 2012*, Nashville, TN, Sept. 17-21, 2012, pp. 2828 - 2849.

[6] EU-U.S. Cooperation on Satellite Navigation, Working Group C, "ARAIM Technical Subgroup Milestone 3 Report," February 25, 2016. Available online at: <http://www.gps.gov/policy/cooperation/europe/2016/working-group-c/>

[7] RTCA Special Committee 159, "Minimum Operational Performance Standards for Airborne

Supplemental Navigation Equipment Using Global Positioning System (GPS)," *RTCA/DO-208*, 1991

[8] Joerger, M., Stevanovic, S., Chan, F.-C., Langel, S., and Pervan, B., "Integrity Risk and Continuity Risk for Fault Detection and Exclusion Using Solution Separation ARAIM," *Proc. of ION GNSS 2013*, Nashville, TN, September 2013.

[9] Joerger, M., Pervan, B., "Fault Detection and Exclusion Using Solution Separation and Chi-Squared RAIM," *Transactions on Aerospace and Electronic Systems*, vol. 52, April 2016, pp. 726-742.

[10] Assistant Secretary of Defense for Command, Control, Communications and Intelligence. "Global Positioning System Standard Positioning Service Performance Standard." Washington, DC, 2008. Available online at <http://www.gps.gov/technical/ps/2008-SPS-performance-standard.pdf>

[11] ICAO, Annex 10, Aeronautical Telecommunications, Volume 1 (Radio Navigation Aids), Amendment 84, published 20 July 2009, effective 19 November 2009.

[12] FAA AC 20-138B, Airworthiness Approval of Positioning and Navigation Systems, September 27, 2010.

[13] Zhai, Y., Joerger, M., Pervan, B., "Continuity and Availability in Dual-Frequency Multi-Constellation ARAIM", *Proc. of ION GNSS+ 2015*, Tampa, FL, Sep 2015, pp. 664-674.

[14] FAA-E-2892d, System Specification for the Wide Area Augmentation System, March 28, 2012

[15] RTCA Special Committee 159, "Minimum Operational Performance Standards for Global Positioning System/Wide Area Augmentation System Airborne Equipment," *Document No. RTCA/DO-229D*. Washington, DC., 2006

[16] T. Walter, J. Blanch, Joerger, M., Pervan, B., "Determination of Fault Probabilities for ARAIM," *Proceedings of IEEE/ION PLANS 2016*, Savannah, GA, April 2016.

[17] Lee, Y., et al., "Summary of RTCA SC-159 GPS Integrity Working Group Activities", *NAVIGATION, Journal of The Institute of Navigation*, Vol. 43, No. 3, Fall 1996, pp. 307-362.

[18] RTCA Special Committee 159, "Minimum Aviation System Performance Standards for the Local Area Augmentation System (LAAS)," *RTCA/DO-245*, 2004, Appendix D.